Ocean Engineering 312 (2024) 118988

Contents lists available at ScienceDirect

Ocean Engineering

journal homepage: www.elsevier.com/locate/oceaneng

Research paper

# Floating solar power loss due to motions induced by ocean waves: An experimental study

Luofeng Huang [a], Yifeng Yang [a,b,*], Danial Khojasteh [c], Binjian Ou [a], Zhenhua Luo [a]

[a] Faculty of Engineering and Applied Sciences, Cranfield University, Cranfield, UK
[b] Department of Mechanical Engineering, University College London, London, UK
[c] School of Civil and Environmental Engineering, University of New South Wales, Sydney, Australia

ARTICLE INFO

*Keywords:*
Floating solar
Wave-induced motions
Tilt angle
Power loss
Solar simulator
Wave tank

ABSTRACT

Whilst there is an interest in floating solar energy systems in coastal and offshore regions to utilise available sea space, they are subject to ocean waves that introduce constant momentum. Consequently, solar panels undergo periodic motions with the waves, causing a continuous change in tilt angle. The tilt angle variation is a sub-optimal process and leads to a loss of energy harnessing efficiency. To investigate this phenomenon, the present study innovatively installed a solar simulator on top of a wave tank. The solar simulator was used to generate high-strength light beams, under which, a floating solar unit was subject to periodic incident waves. Wave-induced motions to the solar system as well as the output power were measured. A systematic analysis of the results indicated that a floating solar unit can have significantly lower power output in waves, compared to its calm-water counterpart. An evident link was established between the wave-induced power loss and the wave-induced rotational movement of the panel. An empirical equation was derived which shows the power loss is predictable through the rotational amplitude. The results also highlight the importance of implementing wave attenuation technologies such as breakwaters to minimise wave-induced motions to floating solar systems. Overall, this research presents a novel experimental approach to assess the difference of floating solar power in ocean-wave versus calm-water scenarios, providing valuable insights for future solar projects on the ocean.

## 1. Introduction

PhotoVoltaic (PV) solar power plants consist of individual solar panels, with which, the power plant scale is flexible as it can be fine-tuned by varying the total number of panels (Sree et al., 2022). This modular approach enables PV systems to be easily installed, cost-effective and adaptable to various scenarios that range from rooftops to utility power plants (Singh, 2013; Zhang et al., 2024). Having such unique advantages, PV has been rapidly deployed and is predicted to become the most used energy technology in the world (IEA, 2022), as shown in Fig. 1(a). PV is currently also the cheapest renewable energy technology in history, and it will likely become even cheaper over time (IRENA, 2020), as shown in Fig. 1(b).

Currently a major obstacle that limits the expansion of solar energy is the availability of suitable space. PV has proven to be an affordable and reliable technology but the energy output is proportional to the covered surface area (Cazzaniga and Rosa-Clot, 2021). Solar panels have primarily been positioned on lands or lakes, but this would occupy precious space which can be utilised for nature conservation and human activities etc. Although over 14,000 GW PV is planned to be installed globally by 2050 (IEA, 2022) (Fig. 1(a)), the availability of space required appears to be a daunting challenge. In this context, the future roadmap to expand solar panels is to extrapolate them from onshore to coastal and offshore, so as to utilise the abundant ocean space (Golroodbari et al., 2021; Shi et al., 2023; Jiang et al., 2023; Esparza et al., 2024). There have been significant industrial actions to implement this roadmap, with numerous ocean-based solar companies developing and testing their prototypes, such as Ocean Sun and HelioRec (Silalahi and Blakers, 2023; Delacroix et al., 2023).

An important performance indicator of solar panels is energy efficiency, which is significantly influenced by the tilt angle, as this dictates the effective area exposed to solar irradiation. There has been a series of studies on the tilt angle effect on the energy efficiency of solar panels. For example, a statistic approach has been used to study the optimal tilt angle of solar panels in different geometric locations (El-Kassaby, 1988; George and Anto, 2012; Kaldellis and Zafirakis, 2012; Kumar et al., 2014; Mamun et al., 2022). Specifically, a series of solar panels were arranged in an area with different tilt angles. The solar energy absorbed over a period of time was used to calculate the energy

* Corresponding author.
*E-mail addresses:* luofeng.huang@cranfield.ac.uk (L. Huang), ucemanj@ucl.ac.uk (Y. Yang).

https://doi.org/10.1016/j.oceaneng.2024.118988
Received 5 July 2024; Received in revised form 9 August 2024; Accepted 10 August 2024
Available online 27 August 2024
0029-8018/© 2024 The Authors. Published by Elsevier Ltd. This is an open access article under the CC BY license (http://creativecommons.org/licenses/by/4.0/).

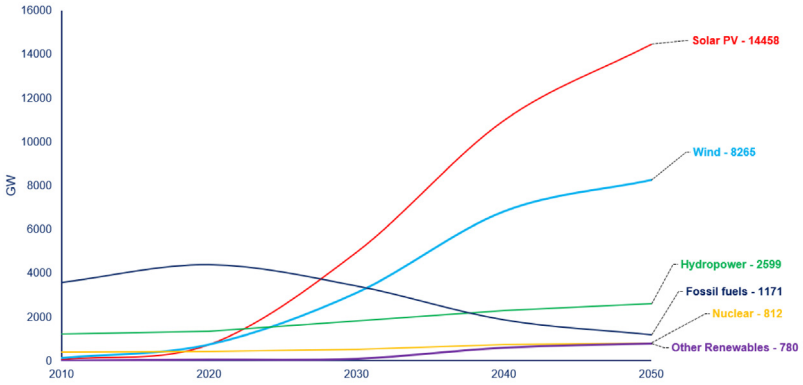


(a) Capacity [4]

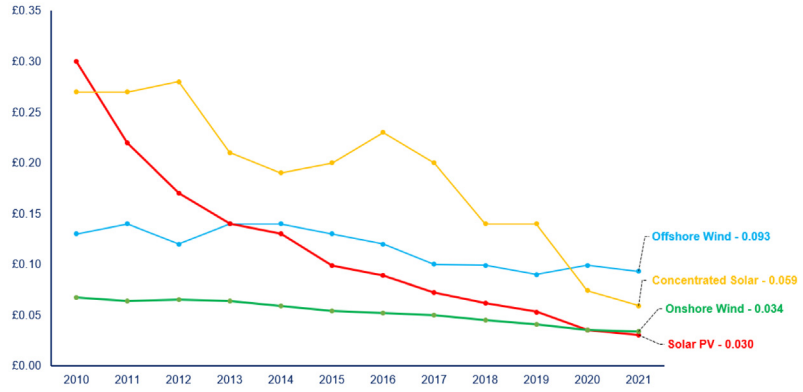


(b) Cost per kWh [5]

**Fig. 1.** World electricity by sources and over time.

efficiency and determine the optimal angle; these types of studies have derived the optimal tilt angles for different latitudes, longitudes and altitudes. Where statistic measurements were unavailable, mathematical modelling has also been applied to predict the optimal tilt angle in a specific condition (Benghanem, 2011; Khatib et al., 2015; Xu et al., 2017; Yunus Khan et al., 2020). Typically, such studies employed the daily or monthly sunlight conditions for a selected location, and then predicted the optimised angle using straightforward equations.

Along with the strong interest in deploying Floating PV (FPV) on seas, the tilt angle can no longer be assessed using the conventional approaches. FPV operating in an oceanic environment faces a significant load from waves, which does not exist for a calm-water condition (e.g. lakes) (Ikhennicheu et al., 2021; Zhang et al., 2023; Yang et al., 2024). Specifically, the wave momentum can induce floating solar panels to rotate continuously, thus the tilt angle will not be fixed (Delacroix et al., 2023; Onsrud, 2019; Sree et al., 2020; Wei et al., 2024b). The varying tilt angle causes the solar panels not to align with incident sunlight at a preferred angle, potentially decreasing the energy efficiency, known as the mismatch effect (Ćatipović et al., 2022).

While the mismatch phenomenon is known to exist, there has been a lack of scientific analysis on how the wave-induced motions of FPV are linked with energy efficiency. Wave tanks and computational simulations are standard approaches for hydrodynamic characteristics, which can be used for predicting wave-induced motions of a floating structure and conducting design optimisations (Zandi et al., 2023, 2024). Nonetheless, contemporary wave tanks do not equip the electrical components necessary to analyse the energy output of a floating solar unit with a varying tilt angle under the influence of wave-induced motions. Based on the above review, the motivation for this work is summarised below:

- Solar panels' power rate is defined in dry conditions. Although there have been studies suggesting that FPV in calm water can have a more than 10% higher efficiency than dry conditions due to water cooling effects (Cazzaniga et al., 2018), there has been no indication of FPV power rate in waves, resulting in inaccuracies in coastal and offshore FPV power prediction.
- Contemporary wave tanks can only test hydrodynamic responses of FPV in waves, missing interdisciplinary abilities to study solar energy that can be influenced by wave-induced motions.
- The relation between FPV's wave-induced motions and power output under a varying tilt angle is unknown.
- Whilst computational simulations can take a large amount of time to perform and will require appropriate experimental data for validation, empirical equations could be derived based on experiments and provided as a quick prediction tool for industrial usage (Huang et al., 2021).
- The design priorities of coastal and offshore FPV have not been clear, e.g. what motion component(s) should be minimised.

The research gap motivated the present work to study the relationship between wave action and FPV power output. To enable such research, the present work developed a new experimental facility to measure FPV motions in various wave conditions, together with its power performance. A solar simulator was installed on top of a wave tank for this purpose, providing energy to an underneath floating solar unit, with power output measured. Then, systematic experiments were conducted and the motion-power relationship was analysed based on the measured data. The novel experimental approach and the results presented are expected to provide insights that will facilitate ocean-based FPV projects to accurately assess potential energy efficiency and enhance future designs. The novelty of this work is outlined below:

- This work innovatively installed a solar simulator on top of a wave tank, which allows energy output variation with wave-induced motions to be measured at the same time.

- The power of FPV in waves in comparison with in calm water is quantified.
- An empirical equation is derived to allow quick prediction and provide insights for conditions not tested in this facility.
- The application of breakwater with floating solar to minimise the wave-induced power loss is discussed.

The paper is organised as follows. Section 2.1 introduces the facilities of a solar simulator installed on a wave tank. Section 2.2 presents the floating solar unit used to test in the newly established interdisciplinary facility. Section 2.3 provides the wave conditions tested, and Section 2.4 details the procedure for calibrations, data collection and analysis. Section 3.1 analyses the motions of the floating solar unit under different wave conditions, and Section 3.2 links the wave-induced motions with the corresponding power output and analyses the relations between them. Section 3.3, based on the experimental data, derives an empirical equation to predict FPV power influenced by waves. Section 3.4 provides design suggestions on how to minimise wave-induced motions for maximising the power output. Finally, Section 4 summarises this research with key conclusions and suggestions for future work.

## 2. Experimental setup

### 2.1. New solar+wave experimental facility

To measure the motion and energy performance of a floating solar structure in waves, a new experimental facility was established at Cranfield University. Specifically, a solar simulator was installed on top of a wave tank, as shown in Fig. 2. The solar simulator can generate high-strength light beams, which can power an underneath solar panel to generate electricity. The solar simulator was assembled by 21 units of Eterna Lighting's CTH500SL 500 W halogen floodlights, arranged as a 7 × 3 matrix to cover the area where the solar panel is placed. The drawings and detailed dimensions of this solar+wave experimental facility are given in Fig. 3.

The wave tank is 30 m long, 1.5 m wide, and filled with freshwater to a depth of 1.5 m. The wave maker uses three physical flappers on one end to produce waves; and on the other end, a physical beach is installed to avoid reflection (Sree et al., 2017; Huang et al., 2019), as presented in Fig. 3(a). The wake marker and physical beach together can generate a prescribed wave field propagating along the wave tank, resembling an open sea environment (Huang et al., 2022). A floating solar unit placed in the tank may move along with the propagating waves. To avoid the FPV from drifting away, a four-pointing mooring approach is used to restrain its horizontal translation, as shown in Figs. 3(b) and 3(c). The wave-induced motions of the floating solar unit can be tracked using accelerometer and inclinometer sensors. Furthermore, the power output of the solar panel was directly recorded through an external cable (visible in Fig. 2). The cable does not influence the FPV motions. In this way, the two interdisciplinary results can be linked and analysed together.

### 2.2. Floating solar unit

The floating solar unit consists of a solar panel and a catamaran floater that lifts the solar panel above the water surface, as shown in Fig. 4. The PV panel is a common commercial type, made by TDG Holding Co., Ltd and the model number is T050M365. It applies the cell technology of Monocrystalline, with a maximum power output of 50 W. Since the solar panel's maximum power rate is 50 W, and solar simulator was adjusted to make the underneath solar panel generate 30 W power on still water. This will be used as a counterpart group for the experiments of FPV power measurement in waves.

The floater possesses a catamaran shape with two hulls, which is newly designed in this work as an alternative to the conventional cuboid shape, helping minimise construction materials. Benefiting from its hydrodynamically superior shape, the catamaran floater takes less wave/current loads than a counterpart cuboid floater, corresponding to less structural movement and less loads transferred to moorings (Jifaturrohman et al., 2024); thus, it is potentially more suitable for an ocean-based FPV project (Zhang et al., 2024). The detailed dimensions of the catamaran are given in Fig. 4. Contemporary floaters are normally made of hollow composite that accounts for a significant part of the cost of the FPV system (Claus and López, 2022); by contrast, the catamaran uses a novel and cheap Extruded Polystyrene (XPS) material, which offers appropriate strength and buoyancy — the XPS has density of 38.44 $\mathrm{kg/m^3}$ and compressive strength of 64.6 psi.

**Table 1**
Tested wave conditions.

| Case number | Wave amplitude (m) | Wave frequency (Hz) | Wavelength (m) |
|---|---|---|---|
| 1 | 0.025 | 1 | 1.561 |
| 2 | 0.025 | 0.95 | 1.730 |
| 3 | 0.025 | 0.9 | 1.927 |
| 4 | 0.025 | 0.85 | 2.160 |
| 5 | 0.025 | 0.8 | 2.437 |
| 6 | 0.05 | 1 | 1.561 |
| 7 | 0.05 | 0.95 | 1.730 |
| 8 | 0.05 | 0.9 | 1.927 |
| 9 | 0.05 | 0.85 | 2.160 |
| 10 | 0.05 | 0.8 | 2.437 |

### 2.3. Testing cases with input wave conditions

In this study, different wave conditions were tested, aiming to create a variety of structural motions as well as energy output. In total, ten periodic wave conditions by a matrix of five periods and two wavelengths were generated and used to test the FPV system. The specific incident wave conditions are given in Table 1. The FPV's power output in calm water was also measured to serve as the counterpart.

The generated waves were periodic sine waves, as illustrated in Fig. 5, which can be specified according to the Stokes wave theory (Dean and Dalrymple, 1991):

$$\eta = h + \frac{H}{2}\cos(kx - \omega t) \tag{1}$$

$$u = \frac{\pi H}{T}\frac{\cosh k(z+h)}{\sinh kh}\cos(kx - \omega t) \tag{2}$$

$$w = \frac{\pi H}{T}\frac{\sinh k(z+h)}{\sinh kh}\sin(kx - \omega t) \tag{3}$$

where $u$ and $w$ are respectively the water velocity components on $x$ and $z$ axes, $\eta$ is the free surface elevation, $H$ is the wave height (twice of wave amplitude $a$), $T$ is the wave period, $k$ is the wave number and $\omega = 2\pi f$ is the angular frequency following wave frequency $f = 1/T$. For the physical wave maker, $H$ and $T$ are given in advance, and the wavelength ($\lambda = 2\pi/k$) was solved by:

$$k\tanh kH = \omega^2/g \tag{4}$$

Eq. (4) describes the dispersion relation that obtains the wave number $k$ through wave height $H$ and wave angular frequency $\omega$ and $g \approx 9.81\ \mathrm{m/s^2}$ is gravitational acceleration.

### 2.4. Data processing

With the periodic waves continuously being generated, propagating, and impacting the FPV, the floating structure starts to undergo periodic motions. Based on the ITTC guidelines (ITTC Quality Manual, 2017), the uncertainty analysis and valid data selection of the present experiments were conducted following the steps below:

**Fig. 2.** Combined solar simulator and wave tank facility at Cranfield University.

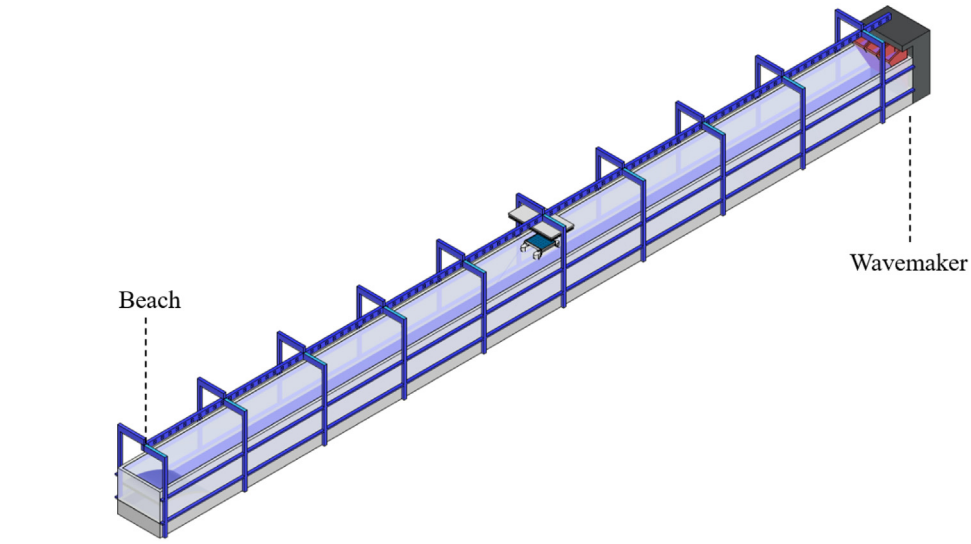


(a) Overview

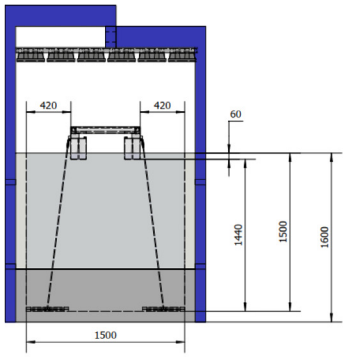


(b) Section view

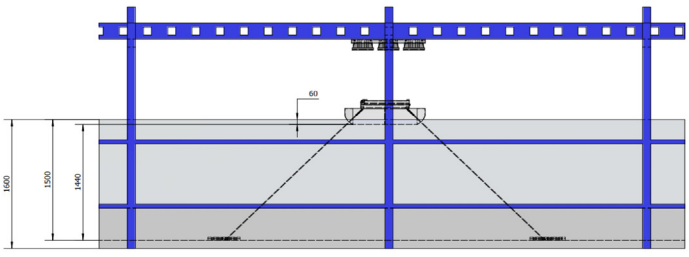


(c) Profile view

**Fig. 3.** Drawings of the solar+wave experimental facility; dimensions in mm.

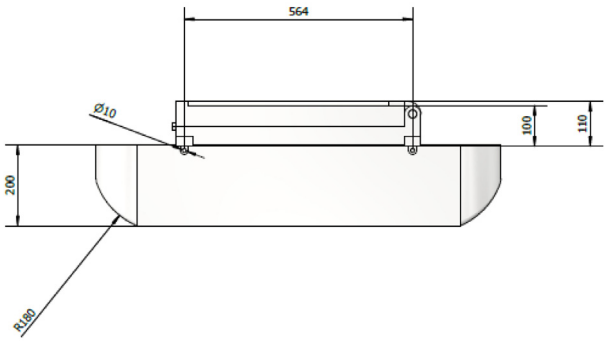


(a) Profile view

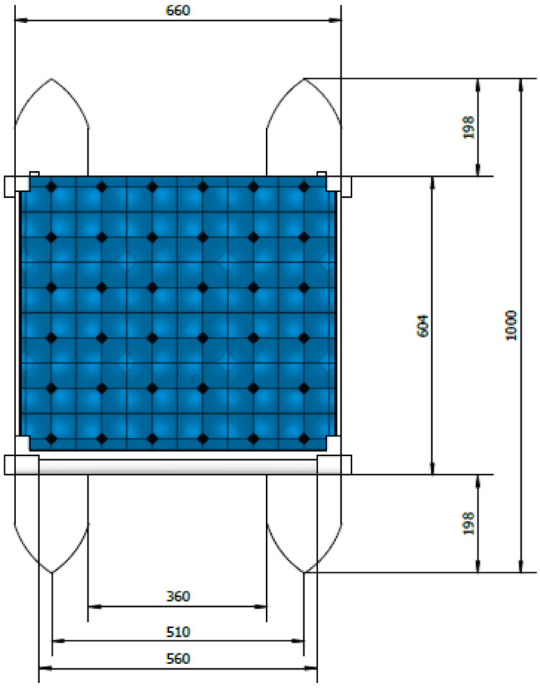


(b) Plan view

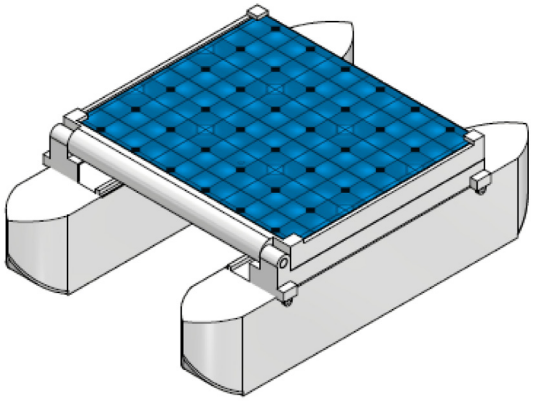

(c) Overview

**Fig. 4.** Drawings of the catamaran floating solar unit; dimensions in mm.

- Calibration: The wave generator and wave gauge were checked before the experiments, by using a ruler to draw ground-truth water levels on the transparent tank wall and compare the results with the digital results measured. Motion sensors were calibrated by moving/rotating them against a ruler/protractor and checking the physical and digital results.
- Receptivity: each experiment was conducted three times and the results were found identical.
- Valid data selection: When the motion sensors show that the motions repeat following wave cycles, the experiment has entered its steady state and then valid data were only taken from this periodic stage. Five repeating wave periods of data were collected and the amplitude was calculated using (the maximum value minus the minimum value) divided by two.

The wave-induced movement was decomposed into translational and rotational motions for analysis. In this particular experiment, the structure mostly conducts a translational motion along the $z$ axis, called heave, and a rotational motion around the $y$ axis, called pitch, as manifested in Fig. 5. The amplitudes of heave and pitch were calculated for analysis, using Eqs. (5) and (6).

$$a_{heave} = (z_{maximum} - z_{minimum})/2 \tag{5}$$

$$a_{pitch} = (\theta_{maximum} - \theta_{minimum})/2 \tag{6}$$

where $z$ is the vertical location for the FPV's centre of gravity, $\theta$ is the rotational angle of the FPV around the $y$ axis, and *maximum* and *minimum* indicate the extremums in a wave cycle.

## 3. Results and discussion

### 3.1. Wave-induced structural motions

The heave and pitch amplitudes of the FPV system in waves are shown in Fig. 6. It can be seen that the heave motion increases with increasing wavelength. Incident waves can be diffracted by the structure which causes the wave to lose its original pattern and the structure cannot heave at the same amplitude as the incident wave (Nelli et al., 2017; Huang and Thomas, 2019). When a wave is sufficiently long (usually when $\lambda$ is more than three times the structural length (Yiew et al., 2016)), the structure is considered relatively small and the incident wave may not be diffracted by the structure; in this scenario, the structure will contour with the waves, shown as heave amplitude equals the wave amplitude. When the wave is relatively short, it is scattered more by the structure, shown as structural heave amplitude decreases with decreasing wavelength.

By contrast, the pitch amplitude result shows to increase with increasing wavelength and then decrease, where the peak value occurred when the wavelength was 1.73 times the structure length. This indicates a relative wavelength corresponding to a wave slope that rotates the structure the most. Similar to heave, when the incident wave is relatively short, it is diffracted by the structure and the structure has small rotations (Yiew et al., 2016); nevertheless, when the incoming wave is too long, without changing the wave height, the wave slope also becomes small and thus the structure has small rotations (Toffoli et al., 2015). Therefore, too short or too long waves do not excite large structural rotations, and there exists a peak amplitude in the pitch motion response to the dominating wavelength. For both heave and pitch, Fig. 6 shows that a larger wave amplitude induces larger structural motions.

In addition to the amplitudes of the motions, an example of the time-series pitch is presented in Fig. 7. In the figure, the first-order and second-order results are obtained by applying the Fourier expansion to the time-series data. This result shows that the second-order component is negligible, confirming that the nonlinearity is weak in this experiment. It suggests that it could be viable to use linear potential-flow

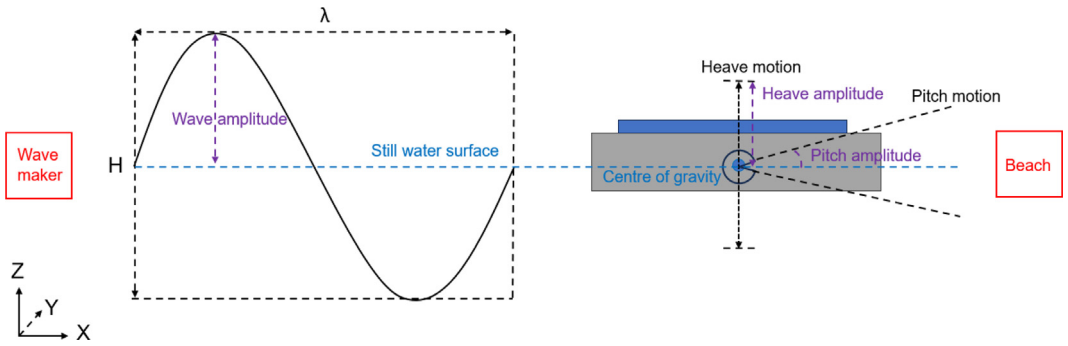


**Fig. 5.** Illustration of the incident waves and the induced structural motions.

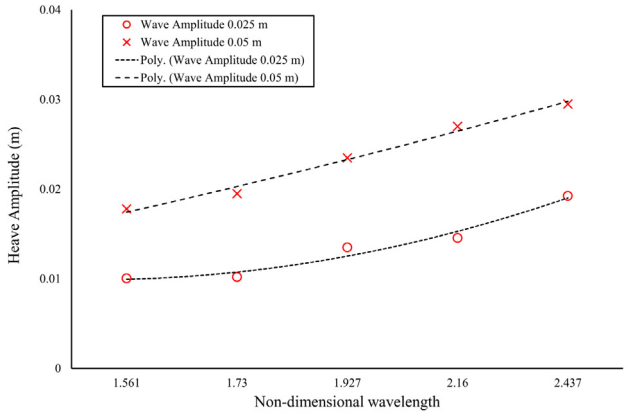


(a) Heave amplitude

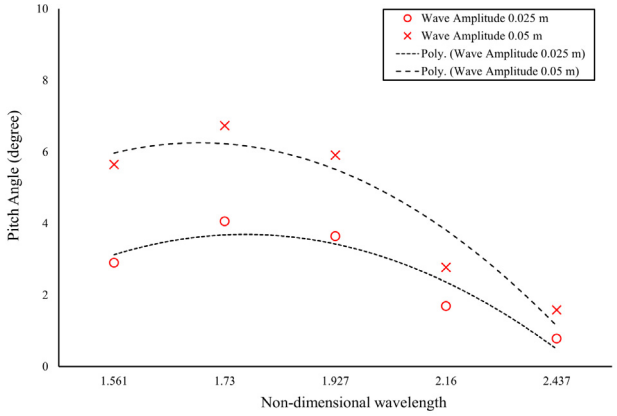


(b) Pitch amplitude

**Fig. 6.** Motion amplitude of the floating solar unit as a function of nondimensional wavelength calculated as $\lambda$ divided by structural length (1 m).

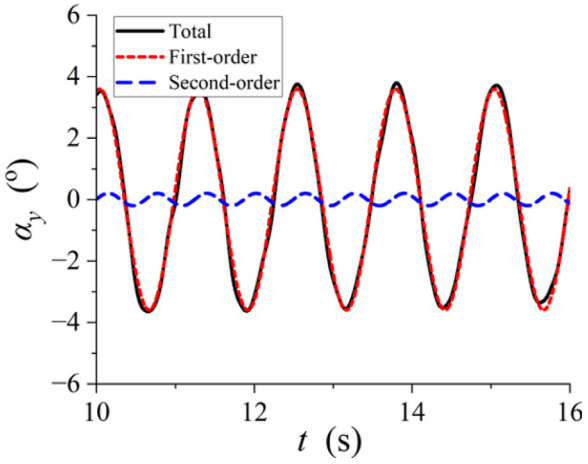


**Fig. 7.** Example of the Fourier expansion of the pitch angle (Case 5).

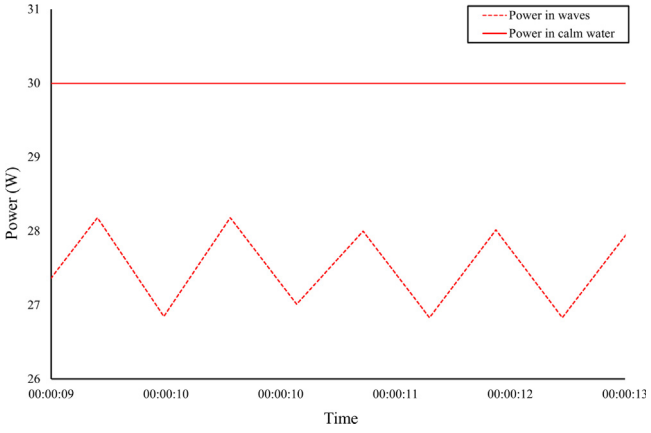


**Fig. 8.** Example of FPV power on calm water and in waves (Case 6).

theories to quickly obtain the motion response (Yang et al., 2024).

### 3.2. FPV power output in waves

The Power output of the FPV fluctuates following the periodic wave-induced motions, which is different from the static performance of an FPV on calm water. Fig. 8 displays an example where the power output exhibits upper and lower limits due to the wave cycle, and the average power output in waves is lower than that on calm water.

As shown in 8, there are upper and lower limits of the power output in each wave cycle. The upper and lower power limits of all tested cases are also plotted in Fig. 9. Correlating to Fig. 6(a), it can be seen that the power oscillation is linked to the heave motion, where a larger heave motion brings about a larger variation between the upper and lower limits. This oscillation can be attributed to the distance between the solar panel and the solar simulator, which is varied by the heave; as the heave motion constantly brings the solar panel closer and farther from the solar simulator, the received light strength alters. In reality, since the distance between a solar panel and the sun is infinite, the influence of heave may be negligible.

Fig. 9 presents the average power output of the FPV in all wave conditions ($PW_{average}$). The average power output is an essential indicator of solar energy as PV panels are exposed to sunlight for a prolonged period of time. It can be seen that wave-induced motions decrease the FPV power output in all cases, compared to the static-water level

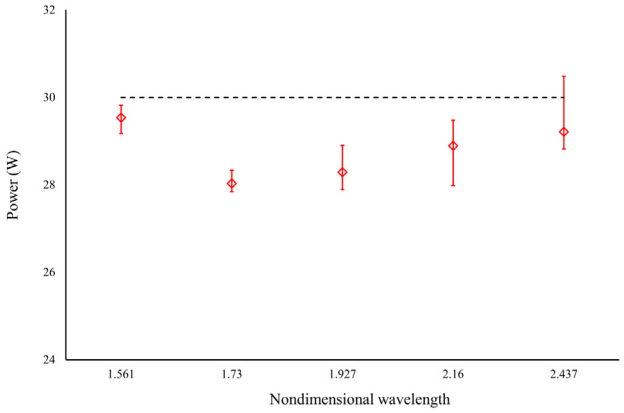


(a) Wave amplitude = 0.025 m

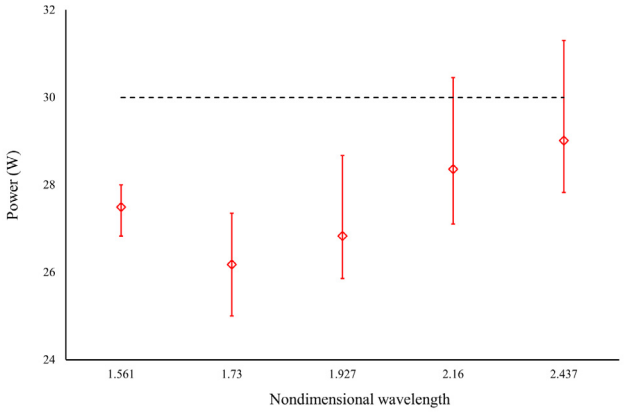


(b) Wave amplitude = 0.05 m

**Fig. 9.** Average power output of FPV in waves, with upper and lower limits in a wave cycle indicated; dash line shows calm-water reference level (no motion)

($PS$). Correlating to Fig. 6(b), it is found that the $PW_{average}$ decreases evidently relating to the pitch motion that causes a misalignment between the solar panel and the light's incident direction. The stronger the pitch motion, the lower the average power for the FPV.

Comparing Figs. 9(a) and 9(b), it is observed that larger wave amplitude will induce larger power oscillation and lower average power. This is in agreement with larger heave and pitch motions shown in Fig. 6. In summary, the rotational pitch motion is found most critical for FPV performance, hence the necessity for engineers to minimise pitch for FPV to have an optimal power performance. This inspires the design of floating support for ocean-based FPV to have a smaller response amplitude operator in pitch (Yiew et al., 2016; Ramachandran et al., 2013).

### 3.3. Empirical equation to predict wave-induced power loss

To provide further insights, the data of pitch amplitude in each wave condition is outlined in Table 2, alongside the Power Loss ($PL$) level calculated by Eq. (7). The power loss is defined as an FPV power amplitude on still water, $PS$, minus its power amplitude in waves, $PW_{average}$, (in %); both $PS$ and $PW_{average}$ were directly measured in the experiments. To enable the prediction of FPV power performance in wave environments, an accurate empirical equation would be particularly valuable. Based on the analysis of sunlight mismatch due to the rotational motion, a hypothesis appears that the $PL$ may be related to certain solar cells that were brought from normal light direction to its tangential, which could be calculated using a *sine* function, written as Eq. (8). $\sin a_{pitch}$ is also given in Table 2, and it was found that the power loss value predicted by $\sin a_{pitch}$ agrees well with the measured. The accuracy level of Eq. (8) is further demonstrated in Fig. 10, and it can be seen that the equation is fairly accurate and obvious inaccuracy only occurs for one case where the measured power loss was very low.

**Table 2**
Data of pitch amplitude and power loss.

| Case number | $a_{pitch}$ (°) | Power loss | $\sin a_{pitch}$ |
|---|---|---|---|
| 1 | 2.9 | 1.5% | 0.050 |
| 2 | 4 | 6.6% | 0.070 |
| 3 | 3.6 | 5.7% | 0.063 |
| 4 | 1.7 | 3.7% | 0.030 |
| 5 | 0.8 | 2.6% | 0.014 |
| 6 | 5.6 | 8.3% | 0.098 |
| 7 | 6.7 | 12.7% | 0.117 |
| 8 | 5.9 | 10.6% | 0.103 |
| 9 | 2.7 | 5.5% | 0.047 |
| 10 | 1.6 | 3.3% | 0.028 |

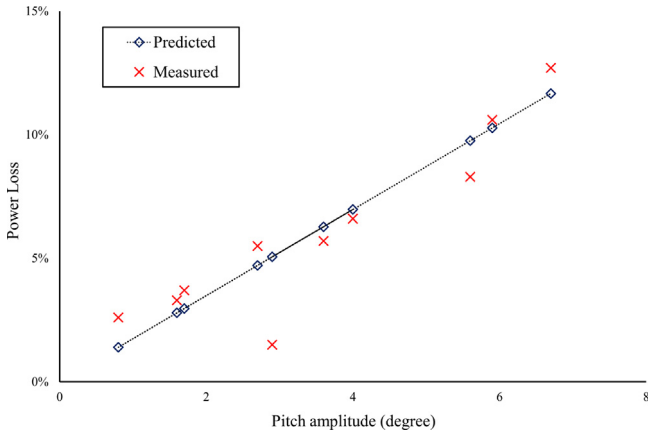


**Fig. 10.** Power loss of FPV in waves: measured in the present experiments and predicted by Eq. (8); raw data can be found in Table 2.

$$PL = (PW_{average} - PS)/PS \times 100\% \tag{7}$$

$$PL = \sin a_{pitch} \tag{8}$$

In practice, for an FPV system with a known power rating on calm water, experiments/simulations/analytics may be used to ascertain its rotational amplitude in waves, and then its power loss due to the dominating wave environment may be predicted by Eq. (8), estimating its power rating on deployed sea conditions; using Eq. (8) in this way can be useful for ocean-based FPV projects, as it fills the contemporary gap to consider FPV power loss due to sea waves.

### 3.4. The application of breakwater with FPV

The highest pitch amplitude in all the measured wave conditions is 6.7°, and this corresponds to a significant level of 12.7% average power loss. This is a limitation of current work as the experimental facility cannot generate high waves as in seas. It will be valuable for future work to examine the power loss when the rotations are large. In reality, the pitch amplitude is expected to be larger than 6.7°, and therefore, more power loss will exist.

To mitigate such power loss for ocean-based solar applications, a wave attenuation technology, e.g. breakwater (Wang et al., 2024), could be applied on the edge of a floating solar farm to avoid direct wave interaction with solar units, as illustrated in Fig. 11. The breakwater will interact with incoming waves, inducing waves to become splashing water and lose continuity (Dai et al., 2018; Wang et al., 2023b). In this way, waves can only radiate a short distance behind

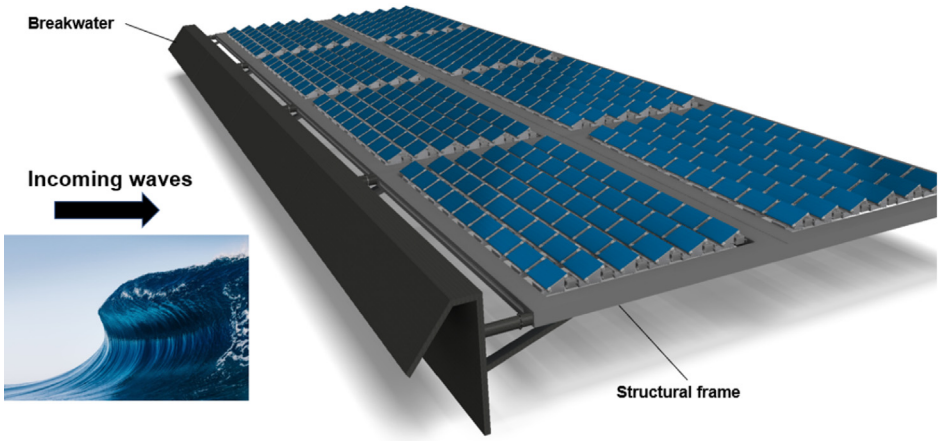


(a) Coastal case

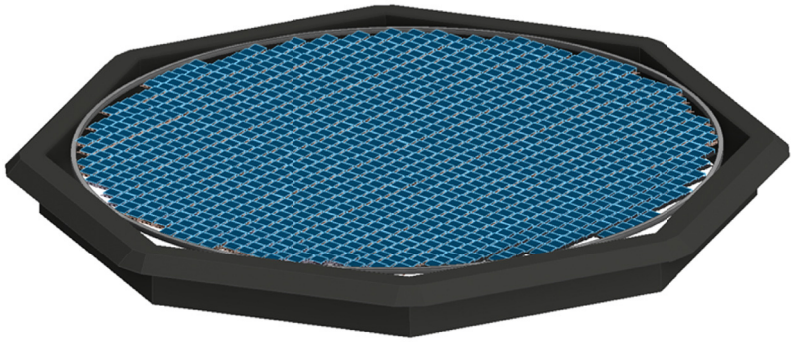

(b) Offshore case

**Fig. 11.** Illustration of breakwater attachment to a floating solar farm.

the breakwater and have minimal interaction with FPV, so as to minimise the pitch motions and power loss. The additional building cost would not be significant with respect to calm-water FPV, as the main additional component is the breakwater in the barrier, i.e. the cost does not increase proportionally with the surface coverage. Thus the larger the surface area of the solar farm, the cheaper the average energy cost will be.

Fig. 11(a) illustrates the case of coastal installation where waves primarily come from one direction. In this case, energy production could also be combined with wider coastal management plans, helping to both reduce carbon emissions and protect coastal populations and assets (Khojasteh et al., 2023; Wang et al., 2023a). For offshore cases, the breakwater would be required to surround the whole solar farm as the offshore waves can come from all directions (Wei et al., 2023), as illustrated in 11(b). The breakwater would also need to be larger than coastal ones to match the offshore sea states. Offshore FPV therefore faces the dilemma between costs and survivability, and the application of breakwater could potentially bring technology breakthroughs and enable large-scale deployments (Zhang et al., 2024; Shi et al., 2023). In addition, wave energy converters could be potentially combined with breakwaters for additional energy harnessing at the same time of wave attenuation (Wei et al., 2024a; Zheng et al., 2024).

## 4. Conclusions

As land and lake-based space may no longer provide enough space to support the global plan to expand solar panel installations, present and future solar projects are looking into deployment on seas. Whilst the ocean space is abundant, the ubiquitous wave can cause FPV to undergo oscillatory rotations so that solar panels may not align with incident sunlight, losing energy efficiency.

To investigate this problem, a new experimental facility was established at Cranfield University, combining a solar simulator with a wave tank. A floating solar unit was designed and built to examine its power output in different wave conditions. Wave-induced motions of the solar unit and the corresponding power fluctuations were measured and analysed. It was found that the pitch motion of a floating solar unit in waves can cause significant power loss compared to the calm-water counterpart. A pitch amplitude of 6.7° can lead to a 12.7% loss of average power, highlighting the importance of minimising the rotation for ocean-based FPV designs.

To enable quick prediction of FPV power loss due to this wave-induced rotation, an empirical equation was derived and it was found that the power loss may be estimated by using a *sine* function. This equation can be useful in practice as it can quickly estimate the power difference of an FPV design on calm water and seas. The paper also highlights the application of breakwaters to minimise wave-induced motions and power loss of FPV. The experimental approach, the analysis of FPV energy variation with waves and its empirical equation, and the application of breakwater with FPV, are novel in this work. Overall, this work provides insights that support ocean-based FPV design, power estimate, and the wider ocean and coastal management plans.

Furthermore, it should be noted that the tested wave conditions were limited by the facility size and thus generally smaller than those in real seas, which means the pitch angles in real life will be bigger and higher energy loss is expected. A way to get around this is to use the

derived empirical equation, which can be inputted with conditions that are not tested. For applications in the real world, if the solar panel's rotational angle in a given wave condition can be estimated, the empirical question can be used to estimate the power loss. Regular waves were used in this study for better parametrisation and analysis, while in the real world, waves will be irregular and therefore it is recommended to use the average response of an FPV in irregular waves for power estimate. In addition, this work is limited to one single panel, while FPVs are normally installed as arrays, and the shading on a solar panel by surrounding panels might be affected by wave-induced motions which could influence the power output. Whilst arranged in arrays, FPVs are connected by joints, where the wave-induced motions will induce fatigue on their joint components, and the associated structural integrity prediction as well as inspection and maintenance plan are valuable for future research.

## CRediT authorship contribution statement

**Luofeng Huang:** Writing – review & editing, Writing – original draft, Visualization, Resources, Project administration, Methodology, Investigation, Funding acquisition, Formal analysis, Data curation, Conceptualization. **Yifeng Yang:** Writing – original draft, Visualization, Methodology, Formal analysis. **Danial Khojasteh:** Writing – review & editing, Investigation. **Binjian Ou:** Visualization, Conceptualization. **Zhenhua Luo:** Resources, Methodology, Funding acquisition, Conceptualization.

## Declaration of competing interest

The authors declare that they have no known competing financial interests or personal relationships that could have appeared to influence the work reported in this paper.

## Data availability

All data underlying the results are available as part of the article and no additional source data are required.

## Acknowledgments

L.H. acknowledges grants received from Innovate UK, United Kingdom (No. 10048187, 10079774, 10081314), the Royal Society, United Kingdom (IEC\NSFC\223253, RG\R2\232462) and UK Department for Transport (TRIG2023 - No. 30066). John Gordon Duffy and Anson Wong from DuPont are much appreciated for providing samples of the XPS material for tests.

## References

Benghanem, Mohamed, 2011. Optimization of tilt angle for solar panel: Case study for madinah, Saudi Arabia. Appl. Energy 88 (4), 1427–1433.

Ćatipović, Ivan, Alujević, Neven, Smoljan, Darko, Mikulić, Antonio, 2022. A review on marine applications of solar photovoltaic systems. In: 15th International Symposium on Practical Design of Ships and Other Floating Structures PRADS 2022.

Cazzaniga, R., Cicu, M., Rosa-Clot, M., Rosa-Clot, P., Tina, G.M., Ventura, C., 2018. Floating photovoltaic plants: Performance analysis and design solutions. Renew. Sustain. Energy Rev. 81, 1730–1741.

Cazzaniga, Raniero, Rosa-Clot, Marco, 2021. The booming of floating PV. Sol. Energy 219, 3–10.

Claus, R., López, M., 2022. Key issues in the design of floating photovoltaic structures for the marine environment. Renew. Sustain. Energy Rev. 112502.

Dai, Jian, Wang, Chien Ming, Utsunomiya, Tomoaki, Duan, Wenhui, 2018. Review of recent research and developments on floating breakwaters. Ocean Eng. 158, 132–151.

Dean, Robert G., Dalrymple, Robert A., 1991. Water wave mechanics for engineers and scientists. vol. 2, World Scientific Publishing Company.

Delacroix, Sylvain, Bourdier, Sylvain, Soulard, Thomas, Elzaabalawy, Hashim, Vasilenko, Polina, 2023. Experimental modelling of a floating solar power plant array under wave forcing. Energies 16 (13), 5198.

El-Kassaby, M.M., 1988. Monthly and daily optimum tilt angle for south facing solar collectors; theoretical model, experimental and empirical correlations. Solar Wind Technol. 5 (6), 589–596.

Esparza, Ignacio, Olábarri Candela, Ángela, Huang, Luofeng, Yang, Yifeng, Budiono, Chayun, Riyadi, Soegeng, Hetharia, Wolter, Hantoro, Ridho, Setyawan, Dony, Utama, IKAP, et al., 2024. Floating PV systems as an alternative power source: Case study on three representative islands of Indonesia. Sustainability 16 (3), 1345.

George, Anu, Anto, Robins, 2012. Analytical and experimental analysis of optimal tilt angle of solar photovoltaic systems. In: 2012 International Conference on Green Technologies. ICGT, IEEE, pp. 234–239.

Golroodbari, S.Z.M., Vaartjes, D.F., Meit, J.B.L., Van Hoeken, A.P., Eberveld, M., Jonker, H., Van Sark, WGJHM, 2021. Pooling the cable: A techno-economic feasibility study of integrating offshore floating photovoltaic solar technology within an offshore wind park. Sol. Energy 219, 65–74.

Huang, Luofeng, Li, Yuzhu, Benites-Munoz, Daniela, Windt, Christian Windt, Feichtner, Anna, Tavakoli, Sasan, Davidson, Josh, Paredes, Ruben, Quintuna, Tadea, Ransley, Edward, et al., 2022. A review on the modelling of wave-structure interactions based on OpenFOAM. OpenFOAM® J. 2, 116–142.

Huang, Luofeng, Li, Zhiyuan, Ryan, Christopher, Ringsberg, Jonas W., Pena, Blanca, Li, Minghao, Ding, Li, Thomas, Giles, 2021. Ship resistance when operating in floating ice floes: Derivation, validation, and application of an empirical equation. Mar. Struct. 79, 103057.

Huang, Luofeng, Ren, Kang, Li, Minghao, Tuković, Željko, Cardiff, Philip, Thomas, Giles, 2019. Fluid-structure interaction of a large ice sheet in waves. Ocean Eng. 182, 102–111.

Huang, Luofeng, Thomas, Giles, 2019. Simulation of wave interaction with a circular ice floe. J. Offshore Mech. Arct. Eng. 141 (4), 041302.

IEA, 2022. World energy outlook 2022. Technical Report.

Ikhennicheu, Maria, Danglade, Benoat, Pascal, Rémy, Arramounet, Valentin, Trébaol, Quentin, Gorintin, Félix, 2021. Analytical method for loads determination on floating solar farms in three typical environments. Sol. Energy 219, 34–41.

IRENA, 2020. How Falling Costs Make Renewables a Cost-effective Investment. Technical Report.

ITTC Quality Manual, 2017. ITTC–recommended procedures and guidelines: Uncertainty analysis for free running model tests (7.5-02-06-05).

Jiang, Zhiyu, Dai, Jian, Saettone, Simone, Tørå, Glenn, He, Zhao, Bashir, Musa, Souto-Iglesias, Antonio, 2023. Design and model test of a soft-connected lattice-structured floating solar photovoltaic concept for harsh offshore conditions. Mar. Struct. 90, 103426.

Jifaturrohman, M.I., Putranto, T., Utama, IK.A.P., Huang, L., 2024. Effect of platform configurations and environmental conditions on the performance of floating solar photovoltaic structures. In: International Marine Design Conference.

Kaldellis, John, Zafirakis, Dimitrios, 2012. Experimental investigation of the optimum photovoltaic panels' tilt angle during the summer period. Energy 38 (1), 305–314.

Khatib, T., Mohamed, Azah, Mahmoud, M., Sopian, Kamaruzzaman, 2015. Optimization of the tilt angle of solar panels for Malaysia. Energy Sources, Part A: Recover. Utiliz. Environ. Effects 37 (6), 606–613.

Khojasteh, Danial, Shamsipour, Abbas, Huang, Luofeng, Tavakoli, Sasan, Haghani, Milad, Flocard, Francois, Farzadkhoo, Maryam, Iglesias, Gregorio, Hemer, Mark, Lewis, Matthew, et al., 2023. A large-scale review of wave and tidal energy research over the last 20 years. Ocean Eng. 282, 114995.

Kumar, Saurav, Chaurasia, P.B.L., Singh, Hari Kumar, 2014. Experimental study of optimum tilt angle for solar PV panel in jaipur (rajasthan). Int. J. Sci. Res. (IJSR) 3 (7), 195–198.

Mamun, M.A.A., Islam, M.M., Hasanuzzaman, M., Selvaraj, Jeyraj, 2022. Effect of tilt angle on the performance and electrical parameters of a PV module: Comparative indoor and outdoor experimental investigation. Energy Built Environ. 3 (3), 278–290.

Nelli, Filippo, Bennetts, L.G., Skene, D.M., Monty, J.P., Lee, J.H., Meylan, M.H., Toffoli, Alessandro, 2017. Reflection and transmission of regular water waves by a thin, floating plate. Wave Motion 70, 209–221.

Onsrud, Magnus, 2019. An Experimental Study on the Wave-Induced Vertical Response of an Articulated Multi-Module Floating Solar Island. NTNU.

Ramachandran, G.K.V., Robertson, Amy, Jonkman, J.M., Masciola, Marco D., 2013. Investigation of response amplitude operators for floating offshore wind turbines. In: ISOPE International Ocean and Polar Engineering Conference. ISOPE, pp. ISOPE–I.

Shi, Wei, Yan, Chaojun, Ren, Zhengru, Yuan, Zhiming, Liu, Yingyi, Zheng, Siming, Li, Xin, Han, Xu, 2023. Review on the development of marine floating photovoltaic systems. Ocean Eng. 286, 115560.

Silalahi, David Firnando, Blakers, Andrew, 2023. Global atlas of marine floating solar PV potential. In: Solar, Vol. 3, No. 3. MDPI, pp. 416–433.

Singh, Girish Kumar, 2013. Solar power generation by PV (photovoltaic) technology: A review. Energy 53, 1–13.

Sree, Dharma K.K., Law, Adrian Wing-Keung, Pang, Dawn Sok Cheng, Tan, Sze Tiong, Wang, Chien Looi, Kew, Jernice Huiling, Seow, Wei Kiong, Lim, Vincent Han, 2022. Fluid-structural analysis of modular floating solar farms under wave motion. Sol. Energy 233, 161–181.

Sree, Dharma K.K., Law, Adrian Wing-Keung, Shen, Hayley H., 2017. An experimental study on the interactions between surface waves and floating viscoelastic covers. Wave Motion 70, 195–208.

Sree, Dharma K.K., Law, Adrian Wing-Keung, Shen, Hayley H., 2020. An experimental study of gravity waves through segmented floating viscoelastic covers. Appl. Ocean Res. 101, 102233.

Toffoli, Alessandro, Bennetts, Luke G., Meylan, Michael H., Cavaliere, Claudio, Alberello, Alberto, Elsnab, John, Monty, Jason P., 2015. Sea ice floes dissipate the energy of steep ocean waves. Geophys. Res. Lett. 42 (20), 8547–8554.

Wang, Chen, Xu, Haochun, Zhang, Yongliang, Chen, Wenchuang, 2023a. Hydrodynamic investigation on a three-unit oscillating water column array system deployed under different coastal scenarios. Coast. Eng. 184, 104345.

Wang, Chen, Xu, Haochun, Zhang, Yongliang, Chen, Wenchuang, 2023b. Power capture analysis of a five-unit oscillating water column array integrated into a breakwater in terms of flow field visualization. Energy Convers. Manage. 293, 117449.

Wang, Chen, Zhang, Yongliang, Xu, Haochun, Chen, Wenchuang, 2024. Multi-stage wave energy conversion and electric power estimation of a chamber-breakwater integrated system with a U-shaped impulse turbine. Energy Convers. Manage. 313, 118591.

Wei, Yujia, Ou, Binjian, Wang, Junxian, Yang, Liang, Luo, Zhenhua, Jain, Sagar, Hetharia, Wolter, Riyadi, Soegeng, Utama, IKAP, Huang, Luofeng, 2023. Simulation of a floating solar farm in waves with a novel sun-tracking system. In: IOP Conference Series: Materials Science and Engineering, Vol. 1288, No. 1. IOP Publishing, 012041.

Wei, Yujia, Yu, Shuangrui, Li, Xiang, Zhang, Chongwei, Ning, Dezhi, Huang, Luofeng, 2024a. Hydrodynamic analysis of a heave-hinge wave energy converter combined with a floating breakwater. Ocean Eng. 293, 116618.

Wei, Yujia, Zou, Detai, Zhang, Deqing, Zhang, Chao, Ou, Binjian, Riyadi, Soegeng, Utama, IKAP, Hetharia, Wolter, Wood, Tim, Huang, Luofeng, 2024b. Motion characteristics of a modularized floating solar farm in waves. Phys. Fluids 36 (3).

Xu, Ruidong, Ni, Kai, Hu, Yihua, Si, Jikai, Wen, Huiqing, Yu, Dongsheng, 2017. Analysis of the optimum tilt angle for a soiled PV panel. Energy Convers. Manage. 148, 100–109.

Yang, Yifeng, Ren, Kang, Zhou, Binzhen, Sun, Shi Yan, Huang, Luofeng, 2024. Wave interaction with multiple adjacent floating solar panels with arbitrary constraints. Phys. Fluids 36 (3).

Yiew, L.J., Bennetts, L.G., Meylan, M.H., French, B.J., Thomas, G.A., 2016. Hydrodynamic responses of a thin floating disk to regular waves. Ocean Model. 97, 52–64.

Yunus Khan, T.M., Soudagar, Manzoore Elahi M., Kanchan, Mithun, Afzal, Asif, Banapurmath, Nagaraj R., Akram, Naveed, Mane, Suresh D., Shahapurkar, Kiran, 2020. Optimum location and influence of tilt angle on performance of solar pv panels. J. Thermal Anal. Calorimetr. 141, 511–532.

Zandi, Reza, Lari, Khosro, Najafzadeh, Mohammad, 2023. Optimum Coastal slopes exposed to waves: Experimental and numerical study. Water 15 (2), 366.

Zandi, Reza, Najafzadeh, Mohammad, Lari, Khosro, Ghazanfari-Moghaddam, Mohammad Sadegh, 2024. Finding the best shape of floating wave energy converters for different primary geometries: Experimental and numerical investigations. Ocean Eng. 307, 118212.

Zhang, Chi, Dai, Jian, Ang, Kok Keng, Lim, Han Vincent, 2024. Development of compliant modular floating photovoltaic farm for coastal conditions. Renew. Sustain. Energy Rev. 190, 114084.

Zhang, Chongwei, Wang, Pengfei, Huang, Luofeng, Zhang, Mengke, Wu, Haitao, Ning, Dezhi, 2023. Resonance mechanism of hydroelastic response of multi-patch floating photovoltaic structure in water waves over stepped seabed. Phys. Fluids 35 (10).

Zheng, Zhi, Jin, Peng, Huang, Qiang, Zhou, Binzhen, Xiang, Ruoxuan, Zhou, Zhaomin, Huang, Luofeng, 2024. Motion response and energy harvesting of multi-module floating photovoltaics in seas. Ocean Eng. 310, 118760.

https://dspace.org/

# Floating solar power loss due to motions induced by ocean waves: an experimental study

**Huang, Luofeng; Yang, Yifeng; Khojasteh, Danial; Ou, Binjian; Luo, Zhenhua**

**2024-11-15**
Elsevier
https://doi.org/10.1016/j.oceaneng.2024.118988
Huang L, Yang Y, Khojasteh D, et al., (2024) Floating solar power loss due to motions induced by ocean waves: an experimental study. Ocean Engineering, Volume 312, Part 1, November 2024, Article number 118988

Downloaded from a DSpace repository. https://dspace.org/